termis.

**Tissue Engineering
& Regenerative Medicine
International Society**

ORIGINAL ARTICLE

Multivalent Conjugates of Sonic Hedgehog Accelerate Diabetic Wound Healing

Bruce W. Han, BS,[1] Hans Layman, PhD,[2] Nikhil A. Rode, MS,[3] Anthony Conway, PhD,[4] David V. Schaffer, PhD,[1,4]
Nancy J. Boudreau, PhD,[2] Wesley M. Jackson, PhD,[1] and Kevin E. Healy, PhD[1,3]

Despite their preclinical promise, few recombinant growth factors have been fully developed into effective therapies, in part, due to the short interval of therapeutic activity after administration. To address this problem, we developed nanoscale polymer conjugates for multivalent presentation of therapeutic proteins that enhance the activation of targeted cellular responses. As an example of this technology, we conjugated multiple Sonic hedgehog (Shh) proteins onto individual hyaluronic acid biopolymers to generate multivalent protein clusters at defined ratios (i.e., valencies) that yield enhanced Shh pathway activation at equivalent concentrations relative to unconjugated Shh. In this study, we investigated whether these multivalent conjugates (mvShh) could be used to improve the therapeutic function of Shh. We found that a single treatment with mvShh significantly accelerated the closure of full-thickness wounds in diabetic (db/db) mice compared to either an equivalent dose of unconjugated Shh or the vehicle control. Furthermore, we identified specific indicators of wound healing in fibroblasts and endothelial cells (i.e., transcriptional activation and cell migration) that were activated by mvShh *in vitro* and at concentrations approximately an order of magnitude lower than the unconjugated Shh. Taken together, our findings suggest that mvShh conjugates exhibit greater potency to activate the Shh pathway, and this multivalency advantage improves its therapeutic effect to accelerate wound closure in a diabetic animal model. Our strategy of multivalent protein presentation using nanoscale polymer conjugates has the potential to make a significant impact on the development of protein-based therapies by improving their *in vivo* performance.

Introduction

GROWTH FACTORS OFFER substantial promise for translation into therapies to promote neovascularization and functional regeneration in ischemic tissues damaged by injury and disease.[1] For decades, laboratory evidence has demonstrated their potent effects on cellular mechanisms of tissue regeneration,[2–4] yet to date, few growth factors have been effectively developed into drug or tissue engineering applications.[5,6] Consistently cited as a limitation to their clinical use is rapid proteolysis and clearance of recombinant growth factors *in vivo*, resulting in an inadequate duration of therapeutic activity after administration.[7–9]

For example, the development of vascular endothelial growth factor (VEGF) was halted in phase II clinical trials, despite its positive safety profile.[10] Due to the short half-life of VEGF ($\sim$30 min[11]), this therapy required frequent administration to yield only a modest effect on neovascularization in injured tissues,[6] and it was deemed unsuitable as a cost-effective drug strategy. Similarly, platelet-derived growth factor (PDGF) is currently approved as a drug to accelerate wound healing, in part, by enhancing cell migration and matrix synthesis.[12] However, due to its even shorter half-life *in vivo* (<2 min[13]), it must be administered at least daily to demonstrate efficacy,[14,15] and therefore, PDGF therapy has not been widely adopted in standard wound management protocols for slowly healing wounds.[16–18] These examples suggest that lengthening the duration of their treatment effect would facilitate the development of new drug therapies based on these and other well-characterized angiogenic growth factors.

A variety of biomaterial and nanotechnology strategies have already demonstrated clinical relevance to improve the stability of recombinant growth factors after administration.[19]

[1]Department of Bioengineering, University of California at Berkeley, Berkeley, California.
[2]Department of Surgery, University of California at San Francisco, San Francisco, California.
Departments of [3]Materials Science and Engineering and [4]Chemical and Biomolecular Engineering, University of California at Berkeley, Berkeley, California.

Encapsulation of proteins into hydrogels, nanoparticles, and micelles is effective to physically sequester them from proteolytic enzymes and can be used to control their release over time.[20,21] A similar strategy uses long-chain polymers composed of polyethylene glycol (PEG) conjugated to the protein-based drug (i.e., PEGylation) to prevent deactivation by immune cells and proteolytic enzymes through steric inhibition.[22] An additional benefit to both of these methods is the ability to modulate the size of the resulting macromolecular entity, thereby enabling control over vascular permeability, tissue diffusion, and elimination routes for the therapeutic growth factor. Other techniques have also been developed to couple recombinant proteins with specific post-translational modifications (e.g., glycosylation[23]) and protein domains (e.g., IgG-Fc[24] and albumin binding[25]), which can improve their solubility and inhibit their systemic elimination. Each of these strategies offers specific advantages to improve protein stability *in vivo*, and the optimal method for a given application will likely depend on the structure of the growth factor, target tissue, and clinical administration requirements.

We have proposed a complementary mechanism to improve the duration of bioactivity for growth factors by increasing their potency. We have generated soluble nanoscale clusters of tethered proteins on single-chain biopolymers using methods that allow for stoichiometric control over the number of proteins on each biopolymer conjugate (i.e., valency). Multivalent presentation of a protein ligand can reduce the overall energy required for multiple ligand binding, as the entropic cost of the first bound ligand brings the conjugate close to the cell surface and generates a discount in entropy required for all subsequent binding events.[26,27] Encouraging these multivalent interactions is equivalent to increasing the local effective concentration of the ligand at the cell surface, which becomes inversely related to the distance between two adjacent ligands along the polymer chain.[28]

We have previously validated methods to effectively measure the valency of these nanoscale protein conjugates,[29] and we have demonstrated that multivalent conjugation of the growth factor Sonic hedgehog (Shh) to linear polymer chains of hyaluronic acid (HyA) yields increasing Shh-pathway activation with higher Shh valencies.[30,31] Furthermore, multivalent Shh conjugates (mvShh) induced enhanced angiogenic function relative to an equivalent dose of unconjugated Shh.[30] Taken together, mvShh conjugates are capable of increasing the per-molecule bioactivity of Shh to elicit therapeutic cellular responses of Shh at lower tissue-level concentrations. Thus, more generally, we propose that although growth factors may be cleared from the target tissues, their therapeutic function can be achieved at lower tissue-level concentrations by employing multivalent conjugates.

In this study, we have extended our previous *in vitro* and *in ovo* findings by investigating how the bioactivity advantage of multivalent conjugation can improve the therapeutic function of Shh using a diabetic wound healing animal model. Each year, more than 10% of the 25 million Americans with diabetes suffer from a difficult-to-heal wound.[32] The diabetic wound healing etiology includes delayed activation of wound healing cells and poor neovascularization of the wound during the proliferative stage of healing.[33] Thus, poor quality tissue substrate is generated with insufficient vascularity for normal skin repair and remodeling,

leading to slow or incomplete healing. The effect of Shh to enhance diabetic wound healing by promoting blood vessel formation and tissue regeneration has been previously characterized[34,35]; although typical of protein-based therapies, the translation of recombinant Shh as a clinical therapeutic has been limited by its short duration of bioactivity *in vivo*.[34]

We hypothesized that multivalent presentation of Shh using mvShh would encourage more rapid healing of diabetic wounds relative to unconjugated Shh due to an enhanced ability to activating cell types that participate in revascularization of the wound bed. We used a murine diabetic mouse model to evaluate how multivalent presentation of Shh enhances its treatment effect on capillary density during early wound healing and on the rate of wound closure. Using *in vitro* assays, we also verified that mvShh activated mechanisms related to revascularization in wound healing cells at lower treatment concentrations relative to unconjugated Shh. This novel strategy of multivalent protein presentation using nanoscale polymer conjugates to improve the pharmacological performance of recombinant growth factors will be an important platform for developing additional protein-based drugs.

Results

Multivalent conjugate characterization

We synthesized mvShh using a previously described two-step conjugation protocol (Fig. 1A).[30] In the first step, we used carbodiimide chemistry to substitute a maleimide reactive group at available carboxylic acids on the HyA biopolymer. In the second step, we combined the maleimide-activated HyA with a cysteine-tagged N-terminal fragment of Shh[36] at prescribed molar feed ratios for multivalent conjugation between the free thiol on the cysteine and maleimide groups on the HyA. By dialysis, we removed the unconjugated protein from the reaction solution and then measured the concentration of conjugated Shh using the bicinchoninic acid (BCA) assay.

We analyzed the mvShh conjugates using size exclusion chromatography (SEC) with continuous in-line monitoring of multiangle light scattering (MALS), differential refractive index (dn/dc), and ultraviolet light absorption (UV), as previously developed in our laboratory.[29] The relative molar mass of Shh protein conjugate increased with increasing ratios of Shh to HyA while maintaining constant HyA weight average molecular weight (Mw) (Fig. 1B), which indicated that the increases in conjugate molar mass could be attributed to increasing Shh valency. Based on this analysis, we used the radius of gyration (Rg,z, see Table 1) to estimate the apparent conjugate radii in physiological solutions, which were in the range of 70–80 nm.

Overall, we observed high efficiency in the conjugation reaction of Shh to HyA. Approximately, 85% of the Shh reacted with the maleimide-activated HyA and remained in the product solution after dialysis. After the reaction, the Mw of HyA in the conjugates was ∼75% of its original value (Fig. 1C). The decrease in the polymer size could be anticipated due to hydrolysis of the ester bond along the HyA backbone as a result of shearing the solution during synthesis, and the change in HyA Mw was consistent between reactions and independent of the conjugation ratio.

FIG. 1. Synthesis and characterization of multivalent Sonic hedgehog (mvShh) conjugates. **(A)** Multivalent conjugation of mvShh was performed using a two-step reaction. **(B)** Analysis of mvShh with size exclusion chromatography with multi-angle light scattering paired with an in-line differential refractometer and ultraviolet spectrometer yielded Mw chromatograms representing Shh protein, hyaluronic acid (HyA), and total conjugate macromolecule. Shh:HyA ratios were calculated using mass fractions as described in the ''Methods'' section (Table 1). **(C)** Approximately 75% of the HyA Mw was retained during the conjugation reactions, and the final HyA Mw was independent of Shh valency, as determined by grouping mvShh on the basis of Shh valency. *Dashed line* indicates initial HyA Mw = 860 kDa. **(D)** Shh valency correlated linearly with the reaction feed concentration of Shh relative to a fixed concentration of HyA (9.4 μM).
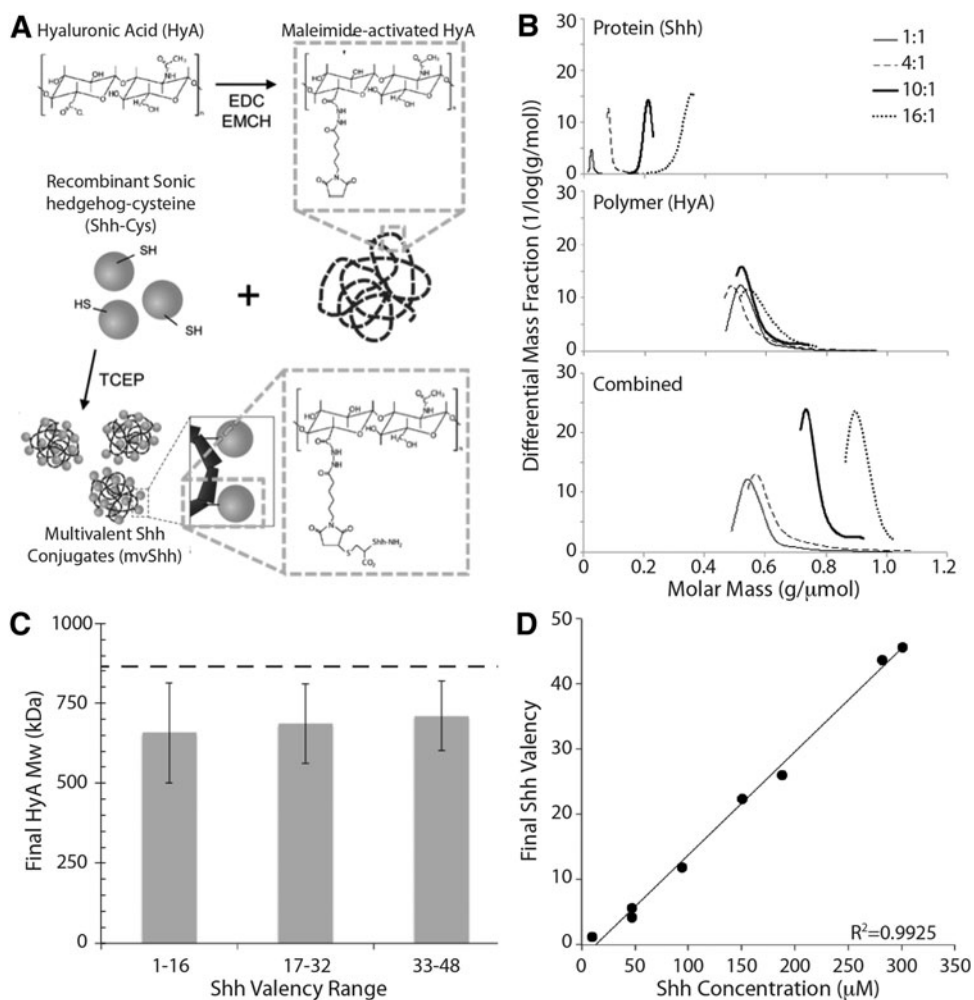
The Shh valency correlated linearly with the reaction feed concentrations over the range of conjugation ratios under consideration in this study (Fig. 1D). We selected mvShh conjugates over a range of Shh valencies to further characterize their bioactivity with *in vivo* and *in vitro* assays.

Assessment of nanoscale polymer conjugates using a diabetic wound healing model

The application of proangiogenic agents do little to improve the already robust wound healing process that occurs in wild-type mice,[37] and thus, a diabetic wound healing model was used to compare the treatment efficacy of mvShh and unconjugated Shh. We generated full-thickness wounds 1 cm in diameter on the dorsal skin of db/db (BKS.Cg-Dock7^{m}+/+Lepr^{db}/J) mice. These mice have a C57 genetic background with a homozygous mutation on the leptin receptor gene, leading to hyperphagia, obesity, and chronic hyperglycemia similar to adult-onset diabetes mellitus type II, and typical blood glucose levels exceeding 350 mg/dL. Furthermore, the db/db mouse is a frequently used model of delayed and diabetic wound healing due to its well-characterized microvascular disease phenotype,[34,38–43] which includes delayed cellular wound infiltration, reduced

TABLE 1. MOLECULAR PARAMETERS FOR MULTIVALENT SONIC HEDGEHOG CONJUGATES USED IN THIS INVESTIGATION

Shh conc. (μM)	Total Mw (kDa)	Shh Mw (kDa)	HyA Mw (kDa)	Fw (Shh:HyA)	Rg,z (nm)	Valency (Shh per HyA)
9.4	567.8	25.4	542.39	0.05	74.1	1
47.0	614.9	88.3	526.57	0.14	76.9	4
75.2	1178.9	250.8	936.2	0.21	100.3	12
141.0	759.7	210.4	549.3	0.28	76.0	10
150.4	1251.1	475.9	817.1	0.37	80.1	22
235.0	911.3	342.9	568.4	0.38	78.0	16
300.8	1757	968.5	788.5	0.55	81.2	46

Shh, Sonic hedgehog; HyA, hyaluronic acid.

angiogenesis, and altered immune function.[44] The aggregate effect of these diabetes-associated impairments includes delayed wound contraction,[41–44] and the average time to complete wound closure in an unsplinted wound is ~50–70% longer in the db/db mice compared to wild-type controls.[41–44] The wounds ($n = 10$) were treated with vehicle control (1% w/v dehydrated methylcellulose [MC]), unconjugated Shh (4.9 μg per wound), or mvShh (4.9 μg Shh per wound and presented with 16:1 valency).

As expected, a fibrin clot formed on all of the wounds within 24 h after the initial surgery, and the initial average wound was $99.25 \pm 17.2 \, \text{mm}^2$. There was no evidence of infection in any of the mice (Fig. 2A, inset). By day 3, the wounds did not demonstrate any substantial decrease in wound area and there were no significant differences in the size of the wounds between treatment groups (Fig. 2A). However, after 7 days, the wounds treated with mvShh were significantly smaller than wounds treated either unconju-

gated Shh or the vehicle controls. The significant reduction in wound area was most evident at day 10 when the wounds treated with mvShh ($30.8 \pm 7.5 \, \text{mm}^2$) were approximately half the size of those treated with unconjugated Shh ($54.1 \pm 14.3 \, \text{mm}^2$), and this improvement persisted through day 17. The mvShh treatment group had an average time to wound closure that was 6.9 days shorter than the vehicle controls (Fig. 2B). Thus, a single treatment of mvShh was effective in substantially improving wound healing that was impaired due to diabetic sequelae, and the treatment effect of mvShh exceeded that of the unconjugated Shh at an equivalent dose.

We assessed epidermal reepithelialization and remodeling of the dermal tissues at day 27 after wounding using histology (Fig. 2C). In all of the groups, a well-defined epidermis extended across the entire wound. The epidermis of the wounds treated with vehicle controls contained multiple layers of hyperproliferative immature cells, which were
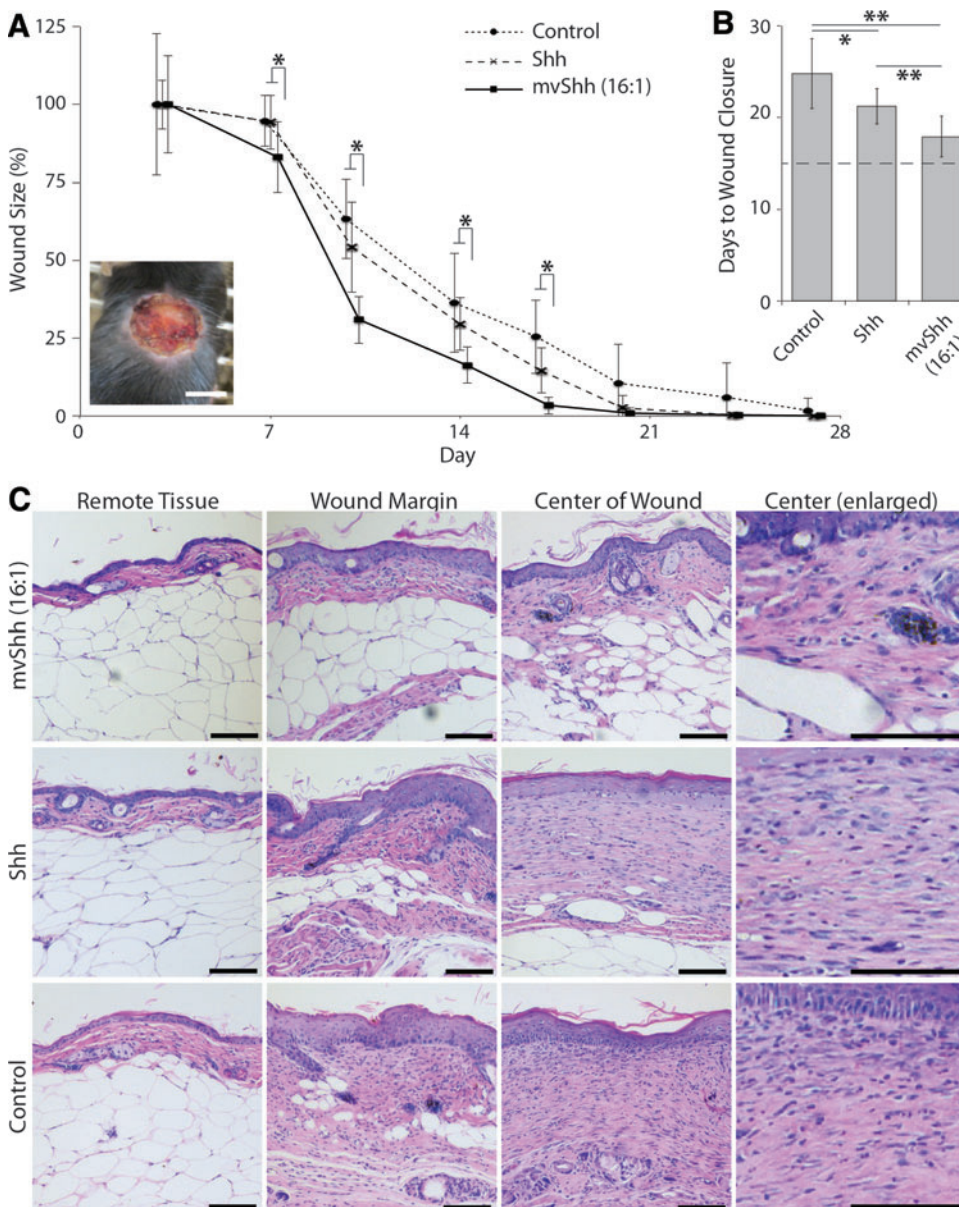

FIG. 2. mvShh treatments decreased the time for wound closure. **(A)** Wounds treated with mvShh were significantly smaller than those treated with Shh or the vehicle control, which was initially detected at day 7 and persisted through day 17 (*$p < 0.05$ between mvShh and both Shh and control, analysis of variance [ANOVA] with $n = 10$). *Inset* image: A representative image of wounds on day 3 that demonstrates wound clotting and no sign of infection in db/db mice. Scale bar = 1 cm. **(B)** mvShh treatment resulted in significantly fewer days to wound closure compared to those treated with unconjugated Shh or vehicle controls. For comparison, the time to wound closure in historical wild-type controls is represented as a *dashed line* (*$p < 0.05$ and **$p < 0.006$, ANOVA with $n = 10$). **(C)** Tissues were harvested at day 27 after wounding. Representative wound cross sections were stained with hematoxylin and eosin to visualize dermal and epidermal thickness at the center of the wound and wound margin compared to the remote tissue for each treatment. Scale bar = 100 μm. Color images available online at www.liebertpub.com/tea

substantially thicker than was observed in the remote skin tissue. By comparison, in both the mvShh and unconjugated Shh treatment groups, the epidermis had thinned to approximately three cell layers, although the width of these cells was still greater than in the remote tissue.

The dermal thicknesses of the wounds treated with the vehicle controls were substantially thicker than in the remote dermis, which is indicative of an active tissue remodeling process.[45] Likewise, the dermis of the wounds treated with unconjugated Shh was nearly as thick as the vehicle controls, suggesting that these wounds were at a similar stage of tissue remodeling. By contrast, the dermal tissue of wounds treated with mvShh appeared to be more mature than those treated with unconjugated Shh, as it had thinned substantially to resemble the remote tissue. Most of the tissue in these mvShh-treated specimens looked similar to the tissue at the wound margin and unwounded remote skin. Thus, the results of this experiment indicate that in addition to accelerating diabetic wound healing relative to unconjugated Shh or vehicles controls, treatment with mvShh conjugates yielded new tissues that more closely resembled unwounded skin.

To further investigate the effect of mvShh on cell function at early stages of wound healing (i.e., 4 and 7 days after wounding), we repeated the experiment using 0.5 cm diameter wounds ($n = 6$) treated with vehicle control, unconjugated Shh (1.2 μg per wound), or mvShh (1.2 μg Shh per wound and presented with 16:1 valency). While the 1 cm wounds were necessary to make reliable wound closure measurements, we refined to our surgical procedure in this experiment to use smaller wounds, as the 0.5 cm size was sufficient to observe the wound in cross section by histology.

We observed wound tissues on days 4 and 7, which corresponded with the initial significant differences in the wound-healing rate between mvShh and unconjugated Shh. After 7 days, the area of wounds treated with the vehicle controls (20.9 ± 4.8 mm^2) appeared similar to those treated with unconjugated Shh (20.5 ± 2.4 mm^2), and those treated with mvShh were significantly smaller (13.1 ± 3.1 mm^2; Fig.

3A, B). These observations followed a similar trend as our wound measurements from the previous experiment, although the effect sizes were not as great owing to the smaller initial wound sizes.

The histological sections at these earlier time points further corroborated the onset of the mvShh treatment effect (Fig. 3C). After 4 days and regardless of the treatment, the epithelial keratinocytes of the epidermis exhibited a cuboidal proliferative morphology, and the dermis was filled with rounded cells, indicating a proliferative and potentially inflamed tissue environment. After 7 days, the epidermal and dermal layers of wounds treated with the vehicle controls appeared similar to those at day 4, suggesting that the wounds had remained at an equivalent phase of wound healing over this period. Similar results were observed in the wounds treated with unconjugated Shh. By comparison, the epidermis of the wounds treated with mvShh appeared thinner and lacking hyperproliferative keratinocytes by day 7. The dermal layer of wounds treated with mvShh also appeared thinner, indicative of progression into the remodeling phase of wound healing.

mvShh enhances cellular mechanisms related to wound healing angiogenesis

To better assess the effect of multivalent Shh presentation on early cellular benchmarks of wound healing, we treated fibroblasts and endothelial cells (ECs) with mvShh and unconjugated Shh *in vitro*. Shh induces angiogenic growth factor expression by fibroblasts (e.g., VEGFs and angiopoietins[46]) downstream of the canonical Shh signaling pathway, which is mediated by the transcriptional factor Gli1.[47] To measure the transcriptional activity of Gli factors, we used ShhLight II reporter cells, which express firefly luciferase (fLuc) under the control of the Gli transcriptional response element in an NIH/3T3 fibroblast background.[48] They also express renilla luciferase (rLuc), constitutively,[49] and thus, by normalizing the fLuc bioluminescence to the
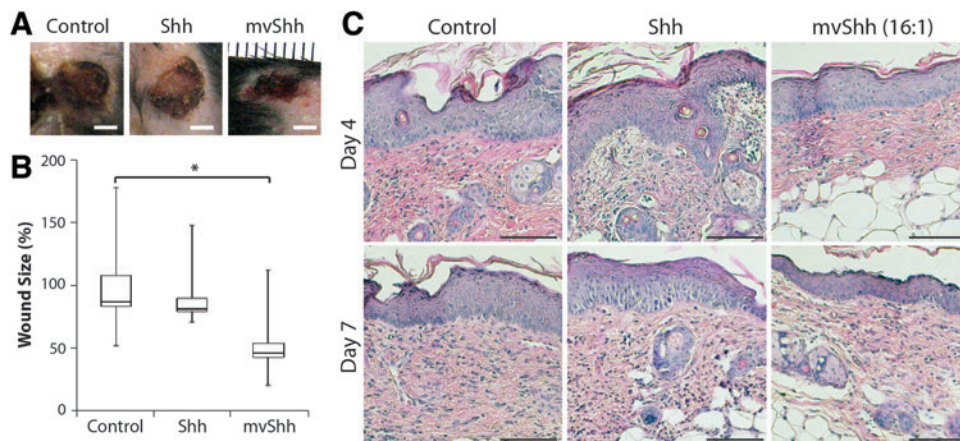

FIG. 3. Evidence of accelerated wound healing was evident at early time points. **(A)** Representative images of 0.5-cm wounds at day 7. Scale bar = 2.5 mm. **(B)** After 7 days, the wounds treated with mvShh (16:1) were smaller than those treated with unconjugated Shh or the vehicle control (*$p < 0.05$ between mvShh and control, Kruskal–Wallis with $n = 6$). **(C)** Representative cross sections of the wounds harvested at days 4 and 7 stained with hematoxylin and eosin to visualize dermal and epidermal thickness. Wounds treated with mvShh demonstrated evidence of resolution by day 7. Scale bar = 100 μm. Color images available online at www.liebertpub.com/tea
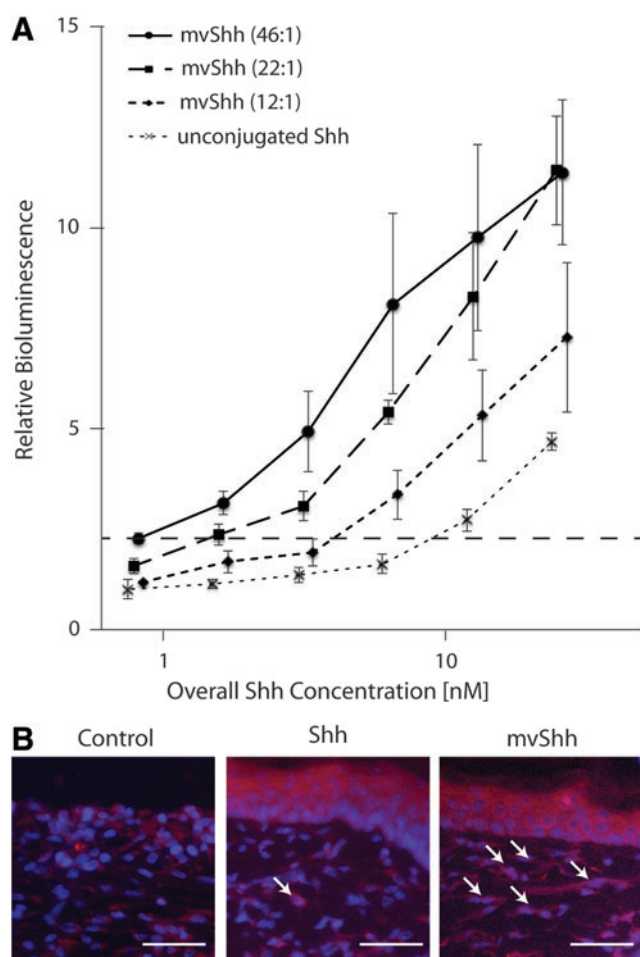
FIG. 4. mvShh activated canonical Shh signaling at lower concentrations relative to unconjugated Shh. **(A)** ShhLight II fibroblasts exhibit valency-dependent increases in Gli1-mediated transcriptional activity. The *dashed line* represents an arbitrary threshold of transcription activation as a means of comparing Shh concentration required to activate the canonical signing for each treatment. **(B)** Gli1 transcriptional activity was detected in the unconjugated Shh and mvShh (16:1)-treated wound cross sections at day 4 using immunohistochemistry. Scale bar $= 50 \mu$m, *arrows* indicate Gli1+ cell staining. Color images available online at www.liebertpub.com/tea

rLuc bioluminescence, we could compare the average cellular transcriptional response generated by mvShh conjugates and unconjugated Shh treatments.

Using this assay system, we determined that the cellular response to mvShh was concentration and valency dependent (Fig. 4A). That is, the magnitude of the transcriptional response at a given treatment concentration of Shh was greater for mvShh conjugates with higher valency. Furthermore, the minimum treatment concentration required to initiate a cellular response was lower for conjugates with higher valency, as the advantage of multiple Shh ligand presentation enhanced the overall conjugate bioactivity. These findings indicate a valency-dependent effect on canonical Shh pathway activation, which is a necessary step in Shh-induced angiogenic function.

To verify the onset of Shh treatment-induced Gli transcriptional activity in cells occupying the wound bed, we stained for Gli1+ cells in the wound tissue specimens using immunohistochemistry (Fig. 4B). Four days after the treatment, Gli1 expressing cells were not readily apparent in the control wounds. However, cells staining positive for Gli1 were present in the wounds from both treatment groups. Thus, any effects of multivalent growth factor presentation to increase the potency of mvShh would also likely contribute to enhanced wound healing through mechanisms that are mediated by Shh-induced signaling *in vivo*.

In addition to canonical Gli signaling, in many cell types, including ECs, the response to Shh is apparently mediated through a nontranscriptional signaling pathway that enhances cytoskeletal motility.[50–52] As a result, the proangiogenic effects of Shh treatment on ECs are typically observed as an increase in their migration, invasion, and tubule formation rates.

We measured the effect of multivalent Shh presentation on C166 murine EC migration using the modified Boyden chamber assay. The number of cells moving across a membrane with 8 μm pores toward Shh or mvShh was dependent on Shh concentration (Fig. 5A), and at 10 nM Shh, $\sim$50% more cells migrated toward the basal chamber when treated with mvShh compared to the unconjugated Shh. The effect of Shh valency was evident for cells moving across a membrane with 3 μm pores (Fig. 5B). The smaller pore size provided greater resistance to cell movement across the membrane, and negligible cell migration occurred in the absence of Shh treatments. In response to an equimolar concentration of 10 nM Shh, the number of migrating cells increased 2–4 times for mvShh relative to the unconjugated Shh and the number of migrating cells also correlated linearly with the Shh valency of the conjugates used in the treatment. These findings further indicate that mvShh conjugates provide valency-dependent enhancement on key Shh-induced functions of ECs that are associated with wound healing.

Finally, we measured the effect of the mvShh treatments directly on wound revascularization using immunohistochemistry to quantify clusters of cells expressing CD31, a cell surface marker for ECs, and to assess the formation of neovascular structures in the wound tissues (Fig. 5C). We found statistical differences in neovascular density between all treatment groups at days 4 and 7 (Fig. 5D). While Shh treatment was sufficient to increase the neovascular density of the wound by day 4, twice as many neovascular structures had formed in the mvShh treatment group compared to unconjugated Shh. The increase in vascular density was likely due, at least in part, to higher migration rate of ECs in response treatment with the mvShh conjugate. Furthermore, the increase in wound vascularization after mvShh treatment was sustained through day 7, providing further evidence that a single treatment of mvShh was sufficient to enhance diabetic wound healing that was prolonged relative to equivalent dose of unconjugated Shh.

Discussion

The *in vivo* concentration of exogenously administered proteins must remain above the therapeutic threshold to impart a treatment effect. In contrast to various proposed
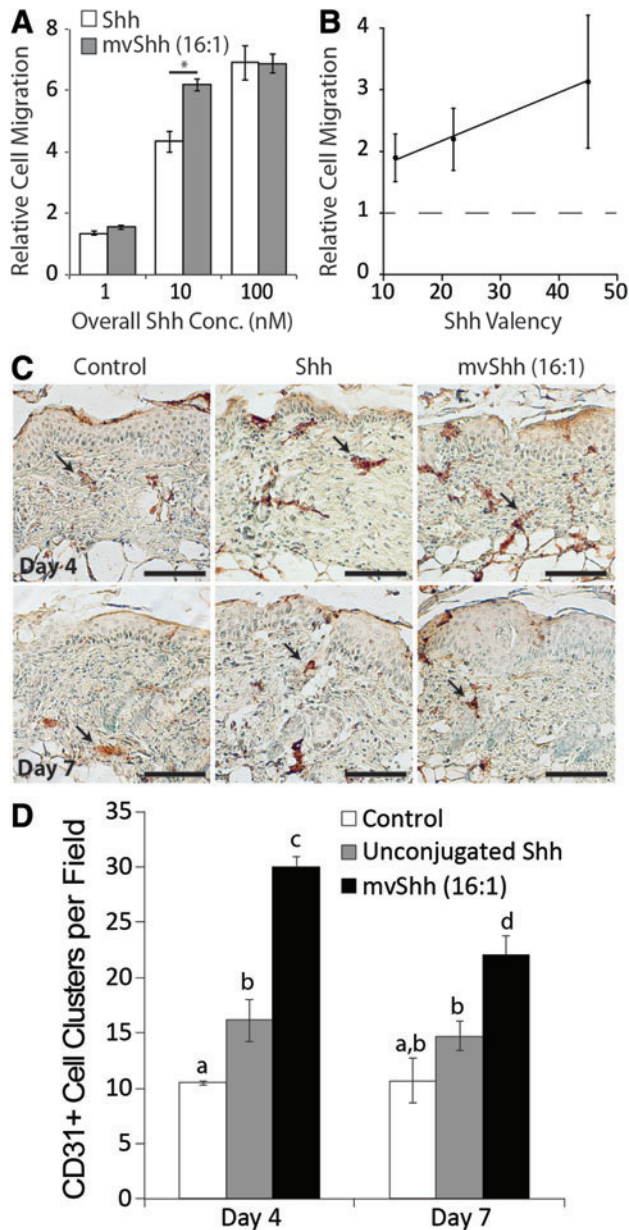
FIG. 5. Shh-induced cellular function was enhanced by mvShh (16:1) relative to unconjugated Shh. **(A)** C166 murine endothelial cells (ECs) treated with mvShh exhibited enhanced migration through 8 μm pores in a modified Boyden Chamber at lower overall Shh concentrations (*$p < 0.05$, Student's t-tests and $n = 4$). 1 = EC invasion in the negative control (0.5% fetal bovine serum). **(B)** Migration through 3 μm pores correlated linearly with Shh valency ($p < 0.05$, t-test on slope with $N = 12$). The number of cells migrating through the pores after treatment with an equimolar dose (10 μM) of unconjugated Shh is represented as a *dashed line*. **(C)** Endothelial migration into the wounds at days 4 and 7 was detected using immunohistochemistry to label the CD31+ cells (*arrows* indicate representative structures). Scale bar = 100 μm **(D)** Quantification of neovascular structures (i.e., cell clusters containing two or more CD31+ cells). Wounds treated with mvShh contained significantly higher numbers of neovascular structures compared to those treated with unconjugated Shh or vehicle controls at both time points (groups that do not share a, b, c, or d: $p < 0.05$, one-way ANOVA with Tukey *post hoc* and $n = 4$). Color images available online at www.liebertpub.com/tea

methods that focus on improving the *in vivo* stability of proteins, we have developed nanoscale polymer conjugates to enable multivalent protein presentation that enhances their potency, thereby lowering the concentration required to activate the target cells. In this study, we have used this strategy to generate multivalent conjugates of Shh to lower the tissue-level protein concentration that would encourage a wound healing response.

We validated our overall hypothesis that diabetic wounds treated with mvShh would heal more rapidly compared to those treated with unconjugated Shh due to its advantage in activating cell types that participate in wound revascularization. We found that wounds treated with vehicle controls required 24.8 ± 3.4 days to heal and unconjugated Shh reduced the healing time by only 3.6 ± 1.9 days. By contrast, administration of the mvShh conjugates nearly doubled the treatment effect by reducing the time to wound closure by 6.9 ± 1.3 days. The mvShh treatments activated important mechanisms related to wound healing angiogenesis in fibroblasts and ECs at *in vitro* concentrations approximately an order of magnitude lower than the unconjugated Shh. We also observed evidence of Shh-induced cellular activation that was sustained for as many as 4 days after wound treatment with mvShh *in vivo*. Finally, the density of neovascular structures identified on the basis of CD31+ cells was approximately two times higher than in those treated with unconjugated Shh and approximately three times higher than in those treated with vehicle controls. Taken together, our findings suggest that mvShh is capable of activating Shh pathways at lower concentrations of Shh, and thus, the increased potency generated by multivalent presentation of Shh contributes to an enhanced therapeutic effect for mvShh to accelerate diabetic wound healing.

Multivalent interactions have been observed widely in various biological systems as a means of improving the affinity and specificity of receptor/ligand binding.[53–55] Work on these interactions has primarily focused on the multivalent receptors that govern the specificity of virus and bacterial identification of host cells, and several studies have taken advantage of this multivalent receptor presentation as a strategy to develop antiviral drugs and inhibitors of bacterial toxins.[56–59] Similar cell–cell interactions between eukaryotic cells, particularly those of the immune system, are enhanced by multivalent antigen presentation to improve the specificity of cell recognition.[60,61] A robust theoretical understanding of these interactions has been developed based on first principles of physical chemistry, polymer mechanics, and biology.[53,62] Mathematical models for this interaction have demonstrated that as ligand valency increases, the entropic barrier for receptor binding decreases with each subsequently bound ligand, and thus, multivalent ligand avidity increases with the ligand valency.[26,27]

These models have been expanded beyond cell adhesion and identity ligands to predict the effect of multivalent growth factors on cellular bioactivity. We have previously reported a numerical solution for mvShh conjugate properties that predict conjugate avidity and Shh pathway activation as a function of Shh valency.[30] Our findings, presented here (Fig. 4A) and previously,[30] were consistent with other studies showing that increasing ligand valency is equivalent to increasing the local effective ligand concentration at the cell surface, which is inversely related to the distance between

two adjacent ligands.[28] Other recent studies have also demonstrated that multivalent presentation of peptide and protein ligands is sufficient to induce enhanced cellular bioactivity relative to an unconjugated monovalent control.[63–65] In a particularly noteworthy study, multivalent conjugates of ephrin-B2-HyA, synthesized using the conjugation protocol described here, demonstrated enhanced differentiation of neural progenitor cells *in vitro* and *in vivo*.[66] In addition, the authors reported that clustering of ephrin-B2 receptors on the cell surface and the downstream pathway activity were correlated directly with ephrin-B2 valency, thereby providing further evidence that the multivalent presentation of protein ligands was sufficient to enhance the activation of their cellular targets.

The wound healing mechanisms of Shh are well characterized and demonstrate how our strategy of multivalent conjugation could be used to enhance the therapeutic effect of an exogenously delivered growth factor. Shh is an important growth and differentiation factor that is required for normal wound healing,[67] and it is produced endogenously as a heparin-bound oligomer to improve its extracellular stability and control over its tissue distribution.[68] Endogenous Shh is a downstream target of hypoxia-induced factor-1α[46] and it promotes adaptive neovascularization in the setting of pathologic tissue ischemia.[69] After exposure to Shh, resident mesenchymal cells regulate a variety of genes with distinct angiogenic functions,[46] including multiple isoforms of VEGF, which promote blood vessel formation, and angiopoietins, which promote vessel branching, stability, and maturity.[70] By a mechanism that appears to involve noncanonical Rho signaling rather than canonical Gli-mediated signaling, Shh also directly stimulates ECs to migrate into the wound bed[52] and encourages their differentiation into tubules.[50–52]

However, the half-life of recombinant Shh *in vivo* is short (<1 h), and the concentration of exogenous Shh diminishes rapidly due to various proteolytic mechanisms.[71] By contrast, as the normal course of treatment, diabetic and slowly healing wounds are treated by standard wound management, which calls for serial debridement and dressing the wounds every 4–7 days.[72,73] Any adjunctive therapies must, therefore, be capable of maintaining their therapeutic activity over multiple days, since the wound dressings should not be removed between clinical visits.[74] Multivalent conjugation of Shh is a novel strategy to improve its therapeutic activity on target cells within the tissue by increasing its potency. Furthermore, as Shh is cleared from the target tissues over time, multivalent conjugation can enable its angiogenic bioactivity at lower tissue-level concentrations relative to unconjugated Shh. Our findings suggest that this effect of multivalent conjugation contributed to accelerated wound healing after treatment with mvShh.

In vivo, conjugation of Shh to HyA also likely contributes to the prolonged bioactivity and overall efficacy of mvShh by resisting the endogenous clearance mechanisms. We have measured the radius of gyration ($R_{g,z}$) of mvShh by SEC-MALS to be ∼70–80 nm in a physiological environment, which is within a range of macromolecular sizes (50–150 nm) that allows movement through the extracellular matrix, but is too large to easily exit the tissue through the circulatory or lymphatic vasculature.[75–77] Conjugation to large macromolecules may also prevent extracellular pro-

teolytic enzymes from accessing Shh,[71,78] thereby increasing the duration of Shh activity *in vivo*. There are also examples from the literature where multivalent conjugation to HyA has been shown to maintain an effective serum concentration of protein-based drugs after systemic administration,[79,80] yielding an improvement in their pharmacokinetics that was comparable to PEGyation.[81] By contrast, in this study, we applied the mvShh treatments locally and were unable to separate the multivalency advantage from any other *in vivo* advantages of conjugation to a long-chain biopolymer.

HyA alone has also been used previously to improve the rate of wound healing, but its efficacy was demonstrated only for doses approximately three orders of magnitude higher than the HyA component of the mvShh treatments used in this study and only when delivered twice daily.[82,83] By contrast, the mvShh provided a therapeutic effect after a single treatment over the 27-day duration of wound healing. Thus, the treatment effect observed in the mvShh group is due to the multivalent conjugation of Shh to HyA, and based on our *in vitro* results, we expect that the bioactivity advantage of mvShh complements any improvement in protein stability associated with conjugation to a long-chain biopolymer.

Conclusions

The use of nanoscale polymer conjugates for multivalent presentation of Shh can significantly enhance the therapeutic efficacy to accelerate wound healing compared to an equivalent concentration of unconjugated Shh. We have demonstrated that multivalent conjugation enhances the potency and therapeutic performance of Shh. Specifically, both Shh-induced transcription and cell migration were activated at lower treatment concentrations of mvShh compared to unconjugated Shh. While the size of the biopolymer conjugates may have had some effect to improve their pharmacokinetics, our findings suggest that the increase in mvShh potency due to multivalent conjugation would also lower the tissue-level concentration required for pathway activation relative to unconjugated Shh. Thus, our method of multivalent conjugation contributed to enhanced therapeutic activity after administration of mvShh in the wound tissue.

It is noteworthy that this novel application of multivalent ligand presentation can be used as a complementary technology with other methods of maintaining an effective therapeutic concentration, such as microencapsulation, *in situ* forming hydrogels, or devices for controlled drug delivery. The multivalent conjugate strategy is also applicable to a wide range of other protein-based drugs that activate their cellular targets through membrane-bound receptors. Therefore, the adoption of multivalent conjugation has the potential to make a significant impact on the development of protein-based therapies by improving their *in vivo* performance.

Methods

Multivalent Shh-HyA conjugate synthesis

We prepared mvShh following a method described previously.[30] Briefly, HyA (Mw ∼860 kDa) was dissolved in 2-(N-morpholino)ethanesulfonic acid buffer (0.1 M, pH 6.5) at 3 mg/mL overnight by gentle stirring. Ten milligram/milliliter

ethyl-3-(3-dimethylaminopropyl)carbodiimide-HCl, 0.3 mg/mL sulfo-NHS, and 1.2 mg/mL maleimidocaproic acid hydrazide were added to the solution and allowed to react for 4 h at 4°C to substitute maleimide reactive groups onto the HyA using a carbodiimide reaction. Samples were dialyzed with 50 kDa MWCO membrane against a phosphate-buffered saline (PBS) buffer (930 mg/L ethylenediaminetetraacetic acid and 10% glycerol in Dulbecco's PBS) once for 4 h and once for 24 h at 4°C. Final concentration of HyA was determined through SEC-MALS. Activated HyA-maleimide was then stored at −20°C for future use. Recombinant N-terminal Shh fragment with an C-terminal cysteine residue was synthesized using an *Escherichia coli* expression system in the QB3 Macrolab (UC Berkeley) using an expression plasmid described previously.[36] Shh-cys was reacted with maleimide-activated HyA in a PBS solution using defined stoichiometric feed ratios at 4°C overnight. The mvShh solution was then dialyzed with 100 kDa MWCO against a PBS buffer once for 4 h and once for 24 h at 4°C. Shh protein conjugation for each mvShh conjugate was measured using the BCA assay (Thermo). Shh valency was measured using SEC with MALS paired with an in-line differential refractometer and ultraviolet spectrometer (SEC-MALS-RI-UV), as described previously.[29] The total molecular mass distribution of the conjugates was determined based on the distribution of light scattering and dn/dc. Then, based on the known dn/dc and UV extinction coefficients (ε_{ex}) for HyA and Shh, we could solve for total dn/dc and UV absorption to determine the Shh and HyA mass fractions over the distribution of total molecular weights. We calculated the Shh valency per HyA macromolecule and final HyA molecular weight based on these mass fractions (Table 1).

Diabetic wound healing model *in vivo*

The IACUC at UCSF approved all animal procedures used in this study. Eight-week-old BKS.Cg-Dock7^m+/+Lepr^{db}/J mice (Jackson Laboratory) were obtained and quarantined for 1 week. Chronic nonfasting hyperglycemia (>350 mg/dL) was verified using a commercial blood glucose monitor, and the animals were randomized into three treatment groups on the basis of blood glucose concentration. The mice were anesthetized with 2.5% isoflurane in oxygen, the dorsum was shaved and sterilized, and then a circle of skin tissue, either 0.5 or 1.0 cm in diameter, was excised from the dorsum to make a full-thickness excisional wound. One of three treatments was applied to each wound through a disk of 1% (w/v) dehydrated methylcellulose (MC) (Sigma Aldrich): mvShh, unconjugated Shh or vehicle saline. Shh (6.25 µg/cm^2) was the treatment dose for both the mvShh and unconjugated treatments. The MC disks were placed directly onto the open wound covering the entire wound. Wound areas were subsequently imaged and measured every 3–4 days by tracing the wounds and calculating the pixel area of each trace with image analysis using ImageJ. Mice were sacrificed at the specified time points by CO_2 asphyxiation.

Histology and immunohistochemistry

Following sacrifice, we performed a bilateral thoracotomy to expose the heart to exsanguinate the carcass with PBS.

Square tissue samples ∼1.5 cm on each side and centered on the wound were excised and cut in half through the diameter of the wound. One half of each wound was fixed in 4% paraformaldehyde, dehydrated, and embedded in paraffin and the other half was embedded with OCT and immediately frozen. The specimens were then sectioned perpendicular to the wound surface at 10 µm intervals and transferred to slides to visualize wound cross sections through the diameter of the wound. At least one slide from each wound was stained with hematoxylin and eosin. We also used the following antibodies for immunohistochemistry: rat anti-mouse CD31 (BD Biosciences) with biotinylated anti-rat IgG and VECTASTAIN Elite ABC Reagent (Vectorlabs) on the paraffin embedded sections, and rabbit anti-mouse Gli1 (Thermo Scientific) with Alexa Fluor-647 conjugated goat anti-rabbit IgG (Invitrogen) on the cryosections. CD31+ cell quantification was performed using previously described methods.[84,85] We imaged the stained cells in the tissue specimens at 20×magnification, which was sufficient to view the full thickness of the epidermis, dermis, and granulation tissues for each specimen. Four nonoverlapping images were required to span the diameter of each wound specimen, and the average cell number per field was calculated for each specimen.

In vitro *translational activation assay*

ShhLight II cells (Johns Hopkins University), a reporter cell line based on 3T3/NIH fibroblasts, were cultured in growth media (GM) containing high-glucose Dulbecco's PBS (DMEM) (Life Technologies) supplemented with 10% bovine calf serum (BCS; ATCC) and 1% penicillin/streptomycin (Life Technologies). Cells were passaged every 3–4 days and never allowed to reach >80% confluency. At the start of the assay, Shh Light II cells were cultured at 20,000 cells/cm^2 in GM, and after ∼3 days, confluent cell cultures were starved for 48 h in DMEM with 0.5% BCS. These media were then replaced by treatment media (DMEM supplemented with 0.5% BCS and mvShh or unconjugated Shh at various concentrations). After incubation for the prescribed time, cells were lysed and the luciferase activity was measured using the Dual-Luciferase Reporter Assay System (Promega) and an IVIS 200 Optical In Vivo Imaging System (Xenogen).

EC migration and invasion assays

C166 ECs (ATCC) were cultured in GM containing high-glucose DMEM (ATCC) supplemented with L-glutamine, 10% fetal bovine serum (FBS; Life Technologies), and 2 mg/mL G418 sulfate (Agilent), and these cells were passaged every 3–4 days. EC migration assays were performed using a modified Boyden chamber system with Fluoroblok inserts and either 8 or 3 µm pores (BD Falcon). C166 cells were starved for 48 h in GM containing 0.5% FBS and then seeded at 100,000 cells/mL on the apical side of the transwell insert. The basal chamber of the insert contained GM with 0.5% and mvShh or unconjugated Shh at various concentrations. After 7 h, the cells in the basal chamber were treated with calcein (Life Technologies) and imaged using a fluorescence microscope (Nikon Eclipse TE300). The number of cells that migrated across the membrane was quantified with ImageJ.

Statistical analysis

The Shapiro–Wilk test for normality was applied to all data. Normally distributed data were represented as mean ± standard deviation, and normally distributed treatment groups were compared using one-way analysis of variance with the Tukey *post hoc* analysis. Non-normally distributed data were represented using box plots with whiskers marking the minimum/maximum values, and non-normally distributed treatment groups were compared using Kruskal–Wallis tests with Dunn's *post hoc* analysis. For all tests, statistical significance was assigned to $p < 0.05$.

Acknowledgments

Funding Sources

Author Contributions

B.W.H.: Performed experimental work, analyzed and interpreted the data, and wrote and edited the manuscript. H.L.: Performed the *in vivo* experimental work, analyzed and interpreted the data, and edited the manuscript. N.A.R.: Performed conjugate analysis, interpreted data, and edited the manuscript. A.C.: Performed multivalent conjugation and analyzed conjugates. D.V.S.: Edited the manuscript. N.J.B.: Supervised the *in vivo* components of this manuscript and edited the manuscript. W.M.J.: Designed the project, analyzed and interpreted the data, intellectually involved in the manuscript, and wrote and edited the manuscript. K.E.H.: Designed the project, analyzed and interpreted the data, supervised the project through all stages, and wrote and edited the manuscript.

Disclosure Statement

K.E.H. and D.V.S. are inventors on a patent application (US2009/038446) associated with this work and owned by the University of California, Berkeley. K.E.H., W.M.J., and D.V.S. own equity interest in Valitor, Inc., which has licensed the technology associated with this work from the University of California, Berkeley.

References

1. Koria, P. Delivery of growth factors for tissue regeneration and wound healing. BioDrugs **26,** 163, 2012.

2. Singer, A.J., and Clark, R.A. Cutaneous wound healing. N Engl J Med **341,** 738, 1999.

3. Barrientos, S., Stojadinovic, O., Golinko, M.S., Brem, H., and Tomic-Canic, M. Growth factors and cytokines in wound healing. Wound Repair Regen **16,** 585, 2008.

4. Behm, B., Babilas, P., Landthaler, M., and Schreml, S. Cytokines, chemokines and growth factors in wound healing. J Eur Acad Dermatol Venereol **26,** 812, 2012.

5. Papanas, N., and Maltezos, E. Growth factors in the treatment of diabetic foot ulcers: new technologies, any promises? Int J Low Extrem Wounds **6,** 37, 2007.

6. Eaglstein, W.H., Kirsner, R.S., and Robson, M.C. Food and Drug Administration (FDA) drug approval end points for chronic cutaneous ulcer studies. Wound Repair Regen **20,** 793, 2012.

7. Pierce, G.F., and Mustoe, T.A. Pharmacologic enhancement of wound healing. Annu Rev Med **46,** 467, 1995.

8. Meyer-Ingold, W. Wound therapy: growth factors as agents to promote healing. Trends Biotechnol **11,** 387, 1993.

9. Johnson, N.R., and Wang, Y. Controlled delivery of sonic hedgehog morphogen and its potential for cardiac repair. PLoS One **8,** e63075, 2013.

10. Hanft, J.R., Pollak, R.A., Barbul, A., van Gils, C., Kwon, P.S., Gray, S.M., Lynch, C.J., Semba, C.P., and Breen, T.J. Phase I trial on the safety of topical rhVEGF on chronic neuropathic diabetic foot ulcers. J Wound Care **17,** 30, 2008.

11. Eppler, S.M., Combs, D.L., Henry, T.D., Lopez, J.J., Ellis, S.G., Yi, J.H., Annex, B.H., McCluskey, E.R., and Zioncheck, T.F. A target-mediated model to describe the pharmacokinetics and hemodynamic effects of recombinant human vascular endothelial growth factor in humans. Clin Pharmacol Ther **72,** 20, 2002.

12. Fang, R.C., and Galiano, R.D. A review of becaplermin gel in the treatment of diabetic neuropathic foot ulcers. Biologics **2,** 1, 2008.

13. Bowen-Pope, D.F., Malpass, T.W., Foster, D.M., and Ross, R. Platelet-derived growth factor *in vivo*: levels, activity, and rate of clearance. Blood **64,** 458, 1984.

14. Smiell, J.M., Wieman, T.J., Steed, D.L., Perry, B.H., Sampson, A.R., and Schwab, B.H. Efficacy and safety of becaplermin (recombinant human platelet-derived growth factor-BB) in patients with nonhealing, lower extremity diabetic ulcers: a combined analysis of four randomized studies. Wound Repair Regen **7,** 335, 1999.

15. Embil, J.M., Papp, K., Sibbald, G., Tousignant, J., Smiell, J.M., Wong, B., and Lau, C.Y. Recombinant human platelet-derived growth factor-BB (becaplermin) for healing chronic lower extremity diabetic ulcers: an open-label clinical evaluation of efficacy. Wound Repair Regen **8,** 162, 2000.

16. Papanas, N., and Maltezos, E. Benefit-risk assessment of becaplermin in the treatment of diabetic foot ulcers. Drug Saf **33,** 455, 2010.

17. Bakker, K., Apelquist, J., Schaper, N.C. and International Working Group on Diabetic Foot Editorial Board. Practical guidelines on the management and prevention of the diabetic foot 2011. Diabetes Metab Res Rev **28,** 225, 2012.

18. Robson, M.C., Steed, D.L., and Franz, M.G. Wound healing: biologic features and approaches to maximize healing trajectories. Curr Probl Surg **38,** 72, 2001.

19. Mahmood, I., and Green, M.D. Pharmacokinetic and pharmacodynamic considerations in the development of therapeutic proteins. Clin Pharmacokinet **44,** 331, 2005.

20. Anitua, E., Sanchez, M., Orive, G., and Andia, I. Delivering growth factors for therapeutics. Trends Pharmacol Sci **29,** 37, 2008.

21. Chen, F.M., Zhang, M., and Wu, Z.F. Toward delivery of multiple growth factors in tissue engineering. Biomaterials **31,** 6279, 2010.

22. Greenwald, R.B., Choe, Y.H., McGuire, J., and Conover, C.D. Effective drug delivery by PEGylated drug conjugates. Adv Drug Deliv Rev **55,** 217, 2003.

23. Sola, R.J., and Griebenow, K. Glycosylation of therapeutic proteins: an effective strategy to optimize efficacy. BioDrugs **24,** 9, 2010.

24. Jazayeri, J.A., and Carroll, G.J. Fc-based cytokines: prospects for engineering superior therapeutics. BioDrugs **22,** 11, 2008.

25. Dennis, M.S., Zhang, M., Meng, Y.G., Kadkhodayan, M., Kirchhofer, D., Combs, D., and Damico, L.A. Albumin binding as a general strategy for improving the pharmacokinetics of proteins. J Biol Chem **277,** 35035, 2002.

26. Krishnamurthy, V.M., Estroff, L.A., and Whitesides, G.M. Multivalency in Ligand Design. Fragment-Based Approaches in Drug Discovery. Weinhein, Germany: Wiley-VCH Verlag GmbH & Co. KGaA, 2006, pp. 11.

27. Kane, R.S. Thermodynamics of multivalent interactions: influence of the linker. Langmuir **26,** 8636, 2010.

28. Kramer, R.H., and Karpen, J.W. Spanning binding sites on allosteric proteins with polymer-linked ligand dimers. Nature **395,** 710, 1998.

29. Pollock, J.F., Ashton, R.S., Rode, N.A., Schaffer, D.V., and Healy, K.E. Molecular characterization of multivalent bioconjugates by size-exclusion chromatography with multiangle laser light scattering. Bioconjug Chem **23,** 1794, 2012.

30. Wall, S.T., Saha, K., Ashton, R.S., Kam, K.R., Schaffer, D.V., and Healy, K.E. Multivalency of Sonic hedgehog conjugated to linear polymer chains modulates protein potency. Bioconjug Chem **19,** 806, 2008.

31. Vazin, T., Ashton, R.S., Conway, A., Rode, N.A., Lee, S.M., Bravo, V., Healy, K.E., Kane, R.S., and Schaffer, D.V. The effect of multivalent Sonic hedgehog on differentiation of human embryonic stem cells into dopaminergic and GABAergic neurons. Biomaterials **35,** 941, 2014.

32. Centers for Disease Control and Prevention. National Diabetes Fact Sheet: National Estimates and General Information on Diabetes and Prediabetes in the United States, 2011. Atlanta, GA: U.S. Department of Health and Human Services, Centers for Disease Control and Prevention, 2011.

33. Falanga, V. Wound healing and its impairment in the diabetic foot. Lancet **366,** 1736, 2005.

34. Asai, J., Takenaka, H., Kusano, K.F., Ii, M., Luedemann, C., Curry, C., Eaton, E., Iwakura, A., Tsutsumi, Y., Hamada, H., Kishimoto, S., Thorne, T., Kishore, R., and Losordo, D.W. Topical sonic hedgehog gene therapy accelerates wound healing in diabetes by enhancing endothelial progenitor cell-mediated microvascular remodeling. Circulation **113,** 2413, 2006.

35. Porro, C., Soleti, R., Benameur, T., Maffione, A.B., Andriantsitohaina, R., and Martinez, M.C. Sonic hedgehog pathway as a target for therapy in angiogenesis-related diseases. Curr Signal Transduct Ther **4,** 31, 2009.

36. Lai, K., Kaspar, B.K., Gage, F.H., and Schaffer, D.V. Sonic hedgehog regulates adult neural progenitor proliferation *in vitro* and *in vivo*. Nat Neurosci **6,** 21, 2003.

37. Hong, Y.K., Lange-Asschenfeldt, B., Velasco, P., Hirakawa, S., Kunstfeld, R., Brown, L.F., Bohlen, P., Senger, D.R., and Detmar, M. VEGF-A promotes tissue repair-associated lymphatic vessel formation via VEGFR-2 and the alpha1beta1 and alpha2beta1 integrins. FASEB J **18,** 1111, 2004.

38. Lerman, O.Z., Galiano, R.D., Armour, M., Levine, J.P., and Gurtner, G.C. Cellular dysfunction in the diabetic fibroblast: impairment in migration, vascular endothelial growth factor production, and response to hypoxia. Am J Pathol **162,** 303, 2003.

39. Hansen, S.L., Young, D.M., and Boudreau, N.J. HoxD3 expression and collagen synthesis in diabetic fibroblasts. Wound Repair Regen **11,** 474, 2003.

40. Mace, K.A., Hansen, S.L., Myers, C., Young, D.M., and Boudreau, N. HOXA3 induces cell migration in endothelial and epithelial cells promoting angiogenesis and wound repair. J Cell Sci **118,** 2567, 2005.

41. Hansen, S.L., Myers, C.A., Charboneau, A., Young, D.M., and Boudreau, N. HoxD3 accelerates wound healing in diabetic mice. Am J Pathol **163,** 2421, 2003.

42. Mace, K.A., Yu, D.H., Paydar, K.Z., Boudreau, N., and Young, D.M. Sustained expression of Hif-1alpha in the diabetic environment promotes angiogenesis and cutaneous wound repair. Wound Repair Regen **15,** 636, 2007.

43. Restivo, T.E., Mace, K.A., Harken, A.H., and Young, D.M. Application of the chemokine CXCL12 expression plasmid restores wound healing to near normal in a diabetic mouse model. J Trauma **69,** 392, 2010.

44. Trousdale, R.K., Jacobs, S., Simhaee, D.A., Wu, J.K., and Lustbader, J.W. Wound closure and metabolic parameter variability in a db/db mouse model for diabetic ulcers. J Surg Res **151,** 100, 2009.

45. Martin, P. Wound healing—aiming for perfect skin regeneration. Science **276**, 75, 1997.

46. Pola, R., Ling, L.E., Silver, M., Corbley, M.J., Kearney, M., Blake Pepinsky, R., Shapiro, R., Taylor, F.R., Baker, D.P., Asahara, T., and Isner, J.M. The morphogen Sonic hedgehog is an indirect angiogenic agent upregulating two families of angiogenic growth factors. Nat Med **7,** 706, 2001.

47. Briscoe, J., and Therond, P.P. The mechanisms of Hedgehog signalling and its roles in development and disease. Nat Rev Mol Cell Biol **14,** 416, 2013.

48. Sasaki, H., Hui, C., Nakafuku, M., and Kondoh, H. A binding site for Gli proteins is essential for HNF-3beta floor plate enhancer activity in transgenics and can respond to Shh *in vitro*. Development **124,** 1313, 1997.

49. Taipale, J., Chen, J.K., Cooper, M.K., Wang, B., Mann, R.K., Milenkovic, L., Scott, M.P., and Beachy, P.A. Effects of oncogenic mutations in Smoothened and Patched can be reversed by cyclopamine. Nature **406,** 1005, 2000.

50. Kanda, S., Mochizuki, Y., Suematsu, T., Miyata, Y., Nomata, K., and Kanetake, H. Sonic hedgehog induces capillary morphogenesis by endothelial cells through phosphoinositide 3-kinase. J Biol Chem **278,** 8244, 2003.

51. Chinchilla, P., Xiao, L., Kazanietz, M.G., and Riobo, N.A. Hedgehog proteins activate pro-angiogenic responses in endothelial cells through non-canonical signaling pathways. Cell Cycle **9,** 570, 2010.

52. Renault, M.A., Roncalli, J., Tongers, J., Thorne, T., Klyachko, E., Misener, S., Volpert, O.V., Mehta, S., Burg, A., Luedemann, C., Qin, G., Kishore, R., and Losordo, D.W. Sonic hedgehog induces angiogenesis via Rho kinase-dependent signaling in endothelial cells. J Mol Cell Cardiol **49,** 490, 2010.

53. Mammen, M., Choi, S.K., and Whitesides, G.M. Polyvalent interactions in biological systems: implications for design and use of multivalent ligands and inhibitors. Angew Chem Int Ed Engl **37,** 2754, 1998.

54. Badjic, J.D., Nelson, A., Cantrill, S.J., Turnbull, W.B., and Stoddart, J.F. Multivalency and cooperativity in supramolecular chemistry. Acc Chem Res **38,** 723, 2005.

55. Kiessling, L.L., Gestwicki, J.E., and Strong, L.E. Synthetic multivalent ligands in the exploration of cell-surface interactions. Curr Opin Chem Biol **4,** 696, 2000.

56. Mammen, M., Dahmann, G., and Whitesides, G.M. Effective inhibitors of hemagglutination by influenza virus synthesized from polymers having active ester groups. Insight into mechanism of inhibition. J Med Chem **38,** 4179, 1995.

57. Mourez, M., Kane, R.S., Mogridge, J., Metallo, S., Deschatelets, P., Sellman, B.R., Whitesides, G.M., and Collier, R.J. Designing a polyvalent inhibitor of anthrax toxin. Nat Biotechnol **19,** 958, 2001.

58. Kitov, P.I., Sadowska, J.M., Mulvey, G., Armstrong, G.D., Ling, H., Pannu, N.S., Read, R.J., and Bundle, D.R. Shiga-like toxins are neutralized by tailored multivalent carbohydrate ligands. Nature **403,** 669, 2000.

59. Matrosovich, M.N., Mochalova, L.V., Marinina, V.P., Byramova, N.E., and Bovin, N.V. Synthetic polymeric sialoside inhibitors of influenza virus receptor-binding activity. FEBS Lett **272,** 209, 1990.

60. Vestweber, D., and Blanks, J.E. Mechanisms that regulate the function of the selectins and their ligands. Physiol Rev **79,** 181, 1999.

61. Schott, E., Bertho, N., Ge, Q., Maurice, M.M., and Ploegh, H.L. Class I negative CD8 T cells reveal the confounding role of peptide-transfer onto CD8 T cells stimulated with soluble H2-Kb molecules. Proc Natl Acad Sci U S A **99,** 13735, 2002.

62. Kitov, P.I., and Bundle, D.R. On the nature of the multivalency effect: a thermodynamic model. J Am Chem Soc **125,** 16271, 2003.

63. Kwon, H.S., Park, J., Park, Y.K., and Ahn, D.R. A multivalent peptide as an activator of hypoxia inducible factor-1alpha. Bioorg Med Chem Lett **23,** 1716, 2013.

64. Gao, X., Qian, J., Zheng, S., Xiong, Y., Man, J., Cao, B., Wang, L., Ju, S., and Li, C. Up-regulating blood brain barrier permeability of nanoparticles via multivalent effect. Pharmaceut Res **30,** 2538, 2013.

65. Swers, J.S., Grinberg, L., Wang, L., Feng, H., Lekstrom, K., Carrasco, R., Xiao, Z., Inigo, I., Leow, C.C., Wu, H., Tice, D.A., and Baca, M. Multivalent scaffold proteins as superagonists of TRAIL receptor 2-induced apoptosis. Mol Cancer Ther **12,** 1235, 2013.

66. Conway, A., Vazin, T., Spelke, D.P., Rode, N.A., Healy, K.E., Kane, R.S., and Schaffer, D.V. Multivalent ligands control stem cell behaviour *in vitro* and *in vivo*. Nat Nanotechnol **8,** 831, 2013.

67. Luo, J.D., Hu, T.P., Wang, L., Chen, M.S., Liu, S.M., and Chen, A.F. Sonic hedgehog improves delayed wound healing via enhancing cutaneous nitric oxide function in diabetes. Am J Physiol Endocrinol Metab **297,** E525, 2009.

68. Vyas, N., Goswami, D., Manonmani, A., Sharma, P., Ranganath, H.A., VijayRaghavan, K., Shashidhara, L.S., Sowdhamini, R., and Mayor, S. Nanoscale organization of hedgehog is essential for long-range signaling. Cell **133,** 1214, 2008.

69. Le, H., Kleinerman, R., Lerman, O.Z., Brown, D., Galiano, R., Gurtner, G.C., Warren, S.M., Levine, J.P., and Saadeh, P.B. Hedgehog signaling is essential for normal wound healing. Wound Repair Regen **16,** 768, 2008.

70. Fujii, T., and Kuwano, H. Regulation of the expression balance of angiopoietin-1 and angiopoietin-2 by Shh and FGF-2. In Vitro Cell Dev Biol Anim **46,** 487, 2010.

71. Pepinsky, R.B., Shapiro, R.I., Wang, S., Chakraborty, A., Gill, A., Lepage, D.J., Wen, D., Rayhorn, P., Horan, G.S., Taylor, F.R., Garber, E.A., Galdes, A., and Engber, T.M. Long-acting forms of Sonic hedgehog with improved pharmacokinetic and pharmacodynamic properties are efficacious in a nerve injury model. J Pharm Sci **91,** 371, 2002.

72. Brem, H., Sheehan, P., and Boulton, A.J. Protocol for treatment of diabetic foot ulcers. Am J Surg **187,** 1S, 2004.

73. Ndip, A., and Jude, E.B. Emerging evidence for neuroischemic diabetic foot ulcers: model of care and how to adapt practice. Int J Low Extrem Wounds **8,** 82, 2009.

74. Tecilazich, F., Dinh, T., and Veves, A. Treating diabetic ulcers. Expert Opin Pharmacother **12,** 593, 2011.

75. Davis, M.E., Chen, Z.G., and Shin, D.M. Nanoparticle therapeutics: an emerging treatment modality for cancer. Nat Rev Drug Discov **7,** 771, 2008.

76. Reddy, S.T., van der Vlies, A.J., Simeoni, E., Angeli, V., Randolph, G.J., O'Neil, C.P., Lee, L.K., Swartz, M.A., and Hubbell, J.A. Exploiting lymphatic transport and complement activation in nanoparticle vaccines. Nat Biotechnol **25,** 1159, 2007.

77. Reddy, S.T., Berk, D.A., Jain, R.K., and Swartz, M.A. A sensitive *in vivo* model for quantifying interstitial convective transport of injected macromolecules and nanoparticles. J Appl Physiol **101,** 1162, 2006.

78. Constantinou, A., Chen, C., and Deonarain, M.P. Modulating the pharmacokinetics of therapeutic antibodies. Biotechnol Lett **32,** 609, 2010.

79. Kong, J.H., Oh, E.J., Chae, S.Y., Lee, K.C., and Hahn, S.K. Long acting hyaluronate—exendin 4 conjugate for the treatment of type 2 diabetes. Biomaterials **31,** 4121, 2010.

80. Yang, J.A., Park, K., Jung, H., Kim, H., Hong, S.W., Yoon, S.K., and Hahn, S.K. Target specific hyaluronic acid-interferon alpha conjugate for the treatment of hepatitis C virus infection. Biomaterials **32,** 8722, 2011.

81. Lee, M.Y., Yang, J.A., Jung, H.S., Beack, S., Choi, J.E., Hur, W., Koo, H., Kim, K., Yoon, S.K., and Hahn, S.K. Hyaluronic acid-gold nanoparticle/interferon alpha complex for targeted treatment of hepatitis C virus infection. ACS Nano **6,** 9522, 2012.

82. Dereure, O., Czubek, M., and Combemale, P. Efficacy and safety of hyaluronic acid in treatment of leg ulcers: a double-blind RCT. J Wound Care **21,** 131, 2012.

83. Voigt, J., and Driver, V.R. Hyaluronic acid derivatives and their healing effect on burns, epithelial surgical wounds, and chronic wounds: a systematic review and meta-analysis

of randomized controlled trials. Wound Repair Regen **20,** 317, 2012.

84. Zhou, Z., Wang, J., Cao, R., Morita, H., Soininen, R., Chan, K.M., Liu, B., Cao, Y., and Tryggvason, K. Impaired angiogenesis, delayed wound healing and retarded tumor growth in perlecan heparan sulfate-deficient mice. Cancer Res **64,** 4699, 2004.

85. Marrotte, E.J., Chen, D.D., Hakim, J.S., and Chen, A.F. Manganese superoxide dismutase expression in endothelial progenitor cells accelerates wound healing in diabetic mice. J Clin Invest **120,** 4207, 2010.

Address correspondence to:
Kevin E. Healy, PhD
Department of Materials Science and Engineering
University of California at Berkeley
Berkeley, CA 94720

E-mail: kehealy@berkeley.edu